Please cite as:
Di Giulio M, Traini T, Sinjari B, Nostro A, Caputi S, Cellini L. Porphyromonas gingivalis biofilm formation ir
surfaces, an in vitro study. Clin Oral Implants Res. 2016 Jul;27(7):918-25. doi: 10.1111/clr.12659. Epub 201
26249670.

Porphyromonas gingivalis biofilm formation in different titanium vitro study

Di Giulio M[1], Traini T[2], Sinjari B[2], Nostro A[3], Caputi S[2], Cellini L[1*].

[1]Department of Pharmacy, University "G. d'Annunzio" Chieti-Pescara, Chieti, Italy.

[2]Department of Medical, Oral and Biotechnological Sciences, University "G. d'Annunzio" Chieti-Pescara

[3]Department of Drug Sciences and Products for Health, University of Messina, Messina, Italy.

*corresponding author: Prof. Luigina Cellini, l.cellini@unich.it

Introduction

Many reasons support the study of the implant surface topographies and their behavior in both in vitro and in vivo conditions.

The implant surface plays a crucial role on osseointegration, as the rate and quality of osseointegration for titanium (Ti) dental implants are related to their surface properties. It was demonstrated that surface composition, hydrophilicity, and roughness are parameters which may play a key role in implant–tissue interaction and osseous integration (Lohmann et al. 2001; Sammons et al. 2005; Zhao et al. 2007). Yet, it has been shown that increasing the three-dimensional topography raises the tensile strength at the bone/implant interface (Buser et al. 1991). Coelho et al. (2009) suggested the use of dental implants with higher surface roughness in regions with low bone density. On the other hand, the increases in the surface roughness result in a subsequent rise of the surface area facilitating the migration and/or retention of pathogens in case of surface colonization.

Laser techniques enable the implant surface treatment without direct contact and provide better control on the micro-topography design. Moreover, the process results in Ti surface microstructures with greatly increased hardness, corrosion resistance, and high degree of purity with a standard roughness and thicker oxide layer (Gaggl et al. 2000; Bereznai et al. 2003). Different studies have indicated more bone formation around laser-treated implants (Li et al. 1997; Cooper 2000; Soboyejo et al. 2002; Faeda et al. 2009).

Cho & Jung (2003) reported an increased removal torque by almost 50% for laser-treated dental implants which was also reported by Faeda et al. (2009), while Hallgren et al. (2003) found a bone/implant contact rate of 40% for the laser-modified implants compared to the 32% of the machined ones.

Although dental implants have become an important option to replace missing teeth, implant failure is still a drawback while periimplant disease is a rising problem facing implantologist (Grossner-Schreiber et al. 2001;€ Elemek & Almas 2014; Hsu et al. 2014).

The development of inflammation around implants (Hallgren et al. 2003; Jung et al. 2008; Zitzmann & Berglundh 2008) is linked to microbial proliferation in a sessile state producing biofilm (Subramani et al. 2009; Dhir 2013; Di Giulio et al. 2013a,b).

It is well known that infections caused by sessile bacteria are characterized both by a strong tolerance to antimicrobial/biocide agents and by an extraordinary resistance to phagocytosis evading the host defences

(Stanley & Lazazzera 2004; Hall-Stoodley & Stoodley 2009). These processes are thought to be the major contributors to the etiology and the persistence of infectious diseases.

Biofilm-growing bacteria represent the cause of exacerbating chronic infections with persistent inflammation and damage of tissue (Jefferson 2004); the biofilm formation on dental implant surface has been considered the main cause of implant failure (Dhir et al. 2006). In cases of peri-implantitis, it has been assumed the association with the putative periodontal pathogens mainly constituted by the bacterial complex, named "red complex" composed of Porphyromonas gingivalis, Tannerella forsythia, Treponema denticola (Quirynen et al. 2002; Lang & Berglundh 2011; Persson & Renvert 2014). Among these bacterial species, P. gingivalis represents the most representative strain involved in severe human periodontitis capable to colonize a variety of host cells producing several virulence factors and also positively interacting with other oral bacterial colonizers (Periasamy & Kolenbrander 2009; Almaguer-Flores et al. 2012; Tribble et al.

2013).

The implant bacterial colonization may occur immediately upon implantation or after osseous integration in the oral cavity. This process is affected by many factors including oral environment, bacterial properties, and material surface characteristics, such as chemical composition, surface energy, hydrophilicity, and topography (Chang & Merritt 1991; Katsikogianni &

Missirlis 2004).

The present study aims to analyze the in vitro effects of the different surface topographies and different implant materials, onto the capability of P. gingivalis to form a microbial biofilm; hence, we assumed a null hypothesis (H0) that different surface preparations and titanium grades have no effects on bacterial biofilm formation.

Material and methods

Substrates

A total of 96 disk-shaped specimens (ø = 6 mm, thickness 2.5 mm) of laser-treated surface (L), sandblasted surface (S), and machined surface (M) of Ti (G4) and Ti-

6Al-4V alloy (G5) (Geass S.r.l., Udine, Italy) were used as substrate materials in this study. The following were the analyzed disks: G4-L, G4-S, G4-M and G5-L, G5-S, G5-M.

Laser-treated surface

The Synthegra treatment (Geass S.r.l.) was based on a controlled micro-ablation of the titanium surface obtained using a Nd–YAG diode-pumped laser operating in Q-switched at low-power setting of the laser beam (less that 1 W) with a very elevated density of energy (tens of GW/cm^2). Pulses are generated over some nanoseconds, concentrating the energy in a few micrometers to produce a surface with thousands of hemispheric pores in less than a minute producing an increase in temperature <1°C.

Sandblasted and machined surfaces The S surface was achieved by grit blasting the Ti surface with either TiO_2 or Al_2O_3 particles ranging in size 25–250 lm. Craters and ridges with a surface roughness (Ra) values placed in the range of 0.5–2.0 lm characterized the resulting surface (Ballo et al. 2011), which is usually anisotropic and occasionally embedded with particles in the surface. The M surface was only turned. The Ra values for M surfaces were been reported in the range of

0.3–1.0 lm (Ballo et al. 2011).

Surface roughness

The roughness average was measured under confocal laser scanning microscope 510 Meta (CLSM) (Zeiss, Jena, Germany) on six specimens. The area of measurement was

1.5 9 1.5 mm, in the central area of the specimens to avoid edge effects. Ra was calculated for each sample as the arithmetic mean of three measurements of the profile points to the average line.

Contact angle

The sessile drop method was used to measure the contact angle. A 2 ll of physiologic saline (NaCl 0.9%) solution drop was carefully placed on each sample surface (G4-L, G4-S, G4-M and G5-L, G5-S, G5-M) using a micro-syringe. The physiologic saline solution was chosen as it is similar to blood plasma in salt composition and osmotic pressure. The measurements were taken at room temperature 23°C (2°C) under constant humidity (45%). The water contact angle (WCA) value was measured from photographs, as the average of the left and right contact angle using a plugin of Image J (1.47 v Wayne Rasband, National Institute of Mental Health, Bethesda, MD, USA). For this detection, a total of six disks, one for each sample surface, were analyzed. The same samples were also used for the evaluation of the surface roughness.

Bacterial strain and culture media

Porphyromonas gingivalis ATCC 33277 was the reference strain used in this study.

The strain was recovered from 80°C in tryptic soy broth supplemented with hemin (0.5 mg/ml; Sigma, Milan, Italy) plus vitamin K (5 mg/ml; Sigma) (TSBHK) and incubated anaerobically at 37°C for 48 h. The broth culture was spread on anaerobe agar base (ABA; Oxoid, Milan, Italy) supplemented with 5% sterile defibrinated horse blood and incubated anaerobically at 37°C for 48–72 h. P. gingivalis colonies were harvested in TSBHK and incubated anaerobically at 37°C for 48 h. After incubation, broth cultures were adjusted to optical density $(O.D.)_{600} = 0.15$ in a spectrophotometer (Eppendorf, Milan, Italy) and used for the experiments.

Experimental design

The effect of different implant surface topographies and materials on the biofilm formation of P. gingivalis was evaluated on 24-well microtiter plates in polystyrene (flat-bottomed tissue-culture-treated plates Nunc, EuroClone SpA, Life-Sciences-Division, Milan, Italy). Sterile disks were placed individually into wells and covered with 1.5 ml of P. gingivalis ATCC 33277 standardized broth culture and incubated anaerobically at 37°C for 48 h.

This experimental procedure was performed for the detection of bacterial biomass, cell viability, concanavalin A assay, and scanning electron microscopy (SEM) evaluation.

Experiments were performed in triplicate.

Biomass assay

The P. gingivalis ATCC 33277 biofilm-forming ability was quantified by safranin staining and by reading the absorbance at 492 nm. After culture incubation, for quantitative measurements, a modified method of Cramton et al. (1999) was used. Briefly, the planktonic bacteria were removed from each well and the sessile bacterial population on disks was washed twice with phosphate-buffered solution (PBS), dried and stained with a 0.1% safranin solution for 1 min, washed with water, and eluted with ethanol. The O.D. of stained biofilms was measured using an enzyme-linked immunosorbent assay (ELISA) reader (SAFAS, Monaco). For this detection, six disks (one for each sample surface) were analyzed with the respective control disks in triplicate for a total of 36 disks.

Cell viability assay

For the evaluation of cells viability, the planktonic cells were removed from each well and the sessile bacterial population on disks was washed with PBS and examined for its viability by Live/Dead BacLight staining (Invitrogen, Milan, Italy) as indicated by manufacturer and observed at fluorescent Leica 4000 DM microscope (Leica Microsystems, Milan, Italy). Images were recorded at an emission wavelength of 500 nm for SYTO 9 (green fluorescence) and of 635 nm for propidium iodide (red fluorescence). Ten fields of view randomly chosen for each disk were examined. For this detection, six disks (one for each sample surface) were analyzed in triplicate for a total of 18 disks.

Concanavalin A assay To visualize the extracellular polymeric substance (EPS) matrix of the biofilms, rhodamine-labeled concanavalin A (rhodamineconA) (Vector Laboratories, Burlingame, CA, USA), which specifically binds to d-(+)-glucose and d-(+)-mannose groups on EPS, was used. After 48 h of incubation, the bacterial planktonic phase was removed from each well and the sessile bacterial population on disks was washed with 1 ml of PBS twice and stained with 50 ll of the rhodamine-conA (10 lg/ml) solution; after a 30 min incubation in the dark at room temperature, the excess staining solution was removed and rinsed with 1 ml of PBS and examined under fluorescence. Images were recorded at an excitation of 514 nm and an emission wavelength of 600 50 nm. For this detection, six disks (one for each sample surface) were analyzed in triplicate for a total of 18 disks.

SEM evaluation
To evaluate the biofilm morphology, the samples were fixed in a 2% solution of glutaraldehyde in 0.1 M PBS for 2 h at 4°C and postfixed for 1 h at 4°C in 1% of osmium tetroxide in the same buffer solution. After thorough washing with PBS, samples were dehydrated in a series of ethanol solutions (30 100%), mounted on aluminum stubs with conductive carbon cement, and vacuum-dried. Samples were subsequently sputter-coated with a gold film (Emitech K 550; Emitech Ltd, Ashford, Kent, UK) and observed under a SEM (Zeiss EVO 50 XVP; Carl Zeiss SMY Ltd, Cambridge, UK) equipped with LaB6 electron gun and an

Everhart–Thornley tetra solid-state detector (4Q-BSD). SEM operating conditions included 10 kV accelerating voltage, 8 mm working distance, and a 10 pA probe current for high vacuum observations and 25 kV accelerating voltage, 8.5 mm working distance, and a 250 pA probe current for observations under variable pressure (0.75 torr). The images were captured with a line average technique using 20 scans. For this detection, six disks (one for each sample surface) were analyzed in triplicate for a total of 18 disks.

Bacterial count by SEM
The bacterial count was performed after 48 h of culture counting the bacterial cells still adherent to specimen surfaces after ultrasound bath (Steroglass S.r.l, Perugia, Italy) treatment of 1 min for three times. A total of four randomly chosen fields for each specimen, treated as above indicated, were imaged under SEM at 20,0009 magnification. The collected images were subsequently measured using an image analysis plugin running under Image J software. Bacteria count was computed using the following equation:

$$Xk¼1 A½lm2 \quad \frac{4}{nb}$$

where n_b was the number of bacteria counted four times and A is the total area imaged at 30,000 K9 magnification measured four times.

Data analysis
Statistical analysis was performed by means of a computerized statistical package (Sigma Stat 3.5, SPSS Inc., Ekrath, Germany). The data, expressed as mean SD, were analyzed with descriptive statistics and normality and equal variance tests to assess whether they had a normal distribution. One-way ANOVA and Holm–Sidak tests were used to evaluate the overall significance and to perform all pairwise comparisons of the mean responses, respectively. A P value of ≤0.05 was considered statistically significant.

Results

The Ra for the L group was 0.10 (0.07) lm inside the craters produced by laser irradiation and 0.40 (0.08) lm in the area limiting the craters; 1.30 (0.61) lm for the S group and finally 0.75 (0.23) lm for the M group (Fig. 1a). The results showed that the L-treated surface appeared to be the smoothest one

($P < 0.05$). The WCA mean (SD) was reported in (Fig. 1b). There were no statistical significant differences between the groups G4 and G5 for each one of the surface treatments (L, S, or M), whereas statistically significant differences ($P < 0.05$) were detected for L, S, and M surface treatments within the same group G4 or G5 in cross-comparisons. The specimens with laser-treated surface showed the highest contact angle.

The effects of different implant surface topographies and materials were evaluated for the P. gingivalis ATCC 33277 biofilm formation capability. Figure 2 showed the P. gingivalis ATCC 33277 produced biofilm on the analyzed surfaces. As shown, statistically significant differences in biofilm formation ($P < 0.001$) were detected among surface topographies on L, S, and M treated G4 disks; in particular, the lowest biomass production was recorded for the L treatment with an absorbance value of 0.38 0.01 and a biomass reduction of 49% and 32% in respect to the M and S disks.

Statistically significant differences ($P < 0.05$) on P. gingivalis ATCC 33277 biofilm formation were recorded on G5-L and G5-S disks when compared to the G5-M disks, with absorbance values of 0.62 0.01 vs. 0.86 0.09 ($P = 0.001$) and 0.63 0.02 vs. 0.86 0.09 ($P = 0.001$), with a biomass reduction of 27.8% and 27.5%, respectively; no difference in biofilm formation was detected between G5-L and G5-S disks.

Regarding the two different detected materials (G4 and G5), significant differences were recorded between G4-L and G5-L ($P < 0.001$) and between G4-M and G5-M ($P = 0.008$), whereas no significant difference in biofilm formation was detected between G4-S and G5-S.

Figure 3 shows the bacterial adhesion on the different surface topographies and materials, focusing the bacterial adhesion and distribution (Fig. 3, left column), the cell

viability (Fig. 3, middle column), and the polysaccharide matrix production (Fig. 3, right column). As shown, both G4-M and G5-M samples (Fig. 3c) displayed a greater overall capability in P. gingivalis attractiveness than the other surface topographies (Fig. 3a,b). In particular, a greater amount of green viable cells (Fig. 3c, middle column) with a massive production of carbohydrates (Fig. 3c, right column) was detected in respect to the other surfaces (Fig. 3a,b, middle and right columns).

The analysis of the total number of adherent bacteria on the different surfaces and materials was shown in Fig. 4. The quantification of the total cells, analyzed counting the different field observed by SEM (representative images were shown in Fig. 4a), showed a significant reduction ($P < 0.01$) on bacterial adhesion on L surfaces in respect to the other treated surfaces (Fig. 4b). No significant difference was recognized when the two materials G4 and G5 were compared to each other (Fig. 4b).

Discussion

The results of the present investigation rejected the hypothesis under test. Statistically significant differences were detected in P. gingivalis biofilm formation for both surface topographies and materials. In particular, within the G4 group, the lowest biomass formation was detected for G4-L with a significant biomass reduction when compared to G4-S and G4-M groups ($P < 0.001$).

Moreover, the numerical results clearly show that the M specimens, erroneously considered as “smooth surface” by clinicians, appear to be much rougher than the lasertreated surface.

Regarding the S surface treatment group, treatment seems to overcome the differences no statistically significant difference was in material composition and reveal a tight noted between G4 and G5 materials; the S relationship between chemistry and surface topography that should be further investigated. Nevertheless, the oxygen-containing compounds at surface level as TiO_2 increase the surface energy. At the same time for hydrophilic surface, an increase in the surface Ra is related to a decrease in the contact angle while for hydrophobic surfaces, an increase in the surface Ra is associated with an increase in the contact angle.

Because the materials and biomaterials placed in the oral cavity interact directly or indirectly with the more than 500 recognized bacterial species (Foster & Kolenbrander 2004; Diaz 2012; Mysak et al. 2014), the relationship between surface of the implant and the red complex bacteria plays an important role (Shibli et al.

2008). It is well known that the biological response around a titanium dental implant depends largely on the chemistry, energy, and topography of its surface (Meyer et al. 2005; Zhao et al. 2006).

The adhesion of bacteria is a process very complex as influenced by the several factors including physicochemical properties of the material surface, surface roughness, hydrophobicity, and surface-free energy. It is known from the literature that surface roughness and hydrophobicity encourage bacterial adhesion. The irregular surfaces provide a larger contact area and retain more bacteria in the hills and valleys than the smooth surfaces protecting from natural removal forces such as salivary fluid flow, tongue, and muscle action. Therefore, it is commonly accepted that smooth surfaces are less likely to be associated with bacterial adhesion (Bollen et al. 1997), particularly a surface with an Ra below 0.2 lm is unlikely to promote microbial adherence due to the larger size of most bacteria (Amoroso et al. 2006).

The L-treated surface appeared to be "smoother" (in mean 0.25 0.15 lm) than the other groups investigated and retained a significant lesser amount of biomass formation. However, the L-treated surface showed a significant higher hydrophobicity (contact angle >90°) and this is apparently in contrast with the statement that hydrophobic surfaces promote the microbial adhesion. However, it must be thought that the contact angle plays an important role in the evaluation of the surface energy: its increase is cause of a decreased surface energy and, interestingly, a decreased surface energy results in a reduced bacterial adhesion (Liu & Zhao 2005).

Indeed, some reports demonstrated that either reduced surface roughness or low surface-free energy materials limit plaque accumulation around an Titanium surfaces exhibit remarkable heterogeneity in physical structure, which depends on chemistry, morphology order, and environment (De Nardo et al. 2012). The L-treated surface of the present study showed an initial hydrophobicity compared to the others surface topographies probably due to the air entrapped in the smallest micro pores created by the laser, leading to a heterogeneous surface, which cannot be spontaneously wetted. On the other hand, it was reported (Rupp et al. 2004) that the surfaces micro-roughness can induce a double effect, an initial hydrophobicity followed by a subsequently enhanced wettability.

In a recent study, Allegrini et al. (2014) underline that the development of new laser treatments, which promote alterations in the surface energy as well as in the macro- and microstructures of Ti, may lead to improved bone-to-implant contact and thus better outcomes.

In this study, the laser-treated surfaces displayed also a reduction in bacterial EPS matrix polysaccharides content, suggesting that a decrease in EPS synthesis might favor the diffusion of drugs into biofilm reducing the antibiotic recalcitrance.

It is widely recognized that an ever-increasing number of infections arise from biofilmproducing microorganisms and that it is strongly difficult to eradicate them. So the best way at the moment appears to be the prevention (reduction) of biofilm formation.

The decrease in bacterial biofilm formation associated with the decrease in both surface energy (>WCA) and surface roughness for G4L here presented confirms the findings of Subramani et al. (2009) who reported an increase in biofilm formation on dental implants where more surface roughness and surface-free energy were found.

The results of the present study, although obtained using one bacterial species, maintain its consistency as the P. gingivalis is a significant periodontal pathogen and one of the microorganisms implicated in peri-implantitis (Shibli et al. 2008). Moreover, belonging to the "red complex", it will serve as starting point to further studies that will be performed including several peri-implant microbiota and host components such as saliva; likewise, it was reported a co-aggregation reaction with T. denticola (Grenier 1992). The obtained results, taking into account the limit of the in vitro study and the use of a monospecies biofilm, encourage to further research in this field including both the use of bacteria clusters and a new co-culture models aimed to mimic the oral environment (Di Giulio et al. 2013b).

Finally, considering the results obtained for bacterial biofilm retention, more weight should be given to the actions of combined factors resulting from time-dependent energy/spatial imbalance as content of oxygen in

the surface layer for a determined surface energy associated with a measured contact angle for an hydrophilic or hydrophobic surface in the presence of different bacteria species. Further research in this field will be addressed to evaluate the same parameters in the presence of bacteria clusters. Conclusions

Within the limits of the present study, the results showed that G4-L appears to be significantly less attractant for the P. gingivalis biofilm formation. The S surface treatment overcomes the differences in material composition without any significant difference in the biofilm formation between G4 and G5. The M surface treatment showed a remarkable increase in the P. gingivalis biofilm formation. The present findings could have a clinical impact. As lesser implant surfaces colonization by P. gingivalis, it may decrease the risk of peri-implant diseases.

Acknowledgements:

Experimental materials and treatments were providedbyGeassS.r.l.Theauthorsacknowledge Emanuela Di Campli and Giovanna Murmura for their valuable support.

Conflict of interest

The authors declare that they have no conflict of interest.

References

Allegrini, S., Jr, Yoshimoto, M., Salles, M.B. & de Almeida Bressiani, A.H. (2014) Biologic response to titanium implants with laser-treated surfaces. The International Journal of Oral & Maxillofacial Implants 29: 63–70.

Almaguer-Flores, A., Olivares-Navarrete, R., Wieland, M., Ximenez-Fyvie, L.A., Schwartz, Z. & Boyan, B.D. (2012) Influence of topography and hydrophilicity on initial oral biofilm formation on microstructured titanium surfaces in vitro. Clinical Oral Implants Research 23: 301– 307.

Amoroso, P.F., Adams, R.J., Waters, M.G. & Williams, D.W. (2006) Williams Titanium surface modification and its effect on the adherence of Porphyromonas gingivalis: an in vitro study. Clinical Oral Implants Research 17: 633–637.

Ballo, A.M., Omar, O., Xia, W. & Palmquist, A. (2011) Dental Implant Surfaces – Physicochemical Properties, Biological Performance, and Trends, Implant Dentistry A Rapidly Evolving Practice. In: Turkyilmaz, I. ed., InTech, Rijeka, Croatia, ISBN: 978-953-307-658-4.

Bereznai, M., Pelsoczi, I., T€ oth, Z., Turz o, K., Rad- nai, M., Bor, Z. & Fazekas, A. (2003) Surface modifications induced by ns and sub-ps excimer laser pulses on titanium implant material. Biomaterials 24: 4197–4203.

Bollen, C.M.L., Lambrechts, P. & Quirynen, M. (1997) Comparison of surface roughness of oral hard materials to the threshold surface roughness for bacterial plaque retention: a review of the literature. Dental Materials 13: 258–269.

Buser, D., Schenk, R.K., Steinemann, S., Fiorellini, J.P., Fox, C.H. & Stich, H. (1991) Influence of surface characteristics on bone integration of titanium implants. A histomorphometric study in miniature pigs. Journal of Biomedical Materials Research 25: 889–902.

Chang, C.C. & Merritt, K. (1991) Effect of Staphylococcus epidermidis on adherence of Pseudomonas aeruginosa and Proteus mirabilis to polymethyl methacrylate (PMMA) and gentamicin-containing PMMA. Journal of Orthopaedic Research 9: 284–288.

Cho, S.A. & Jung, S.K. (2003) A removal torque of the laser-treated titanium implants in rabbit tibia. Biomaterials 24: 4859–4863.

Coelho, P.G., Granjeiro, J.M., Romanos, G.E., Suzuki, M., Silva, N.R., Cardaropoli, G., Thompson, V.P. & Lemons, J.E. (2009) Basic research methods and current trends of dental implant surfaces. Journal of Biomedical Materials Research Part B: Applied Biomaterials 88: 579–596.

Cooper, L.F. (2000) A role for surface topography in creating and maintaining bone at titanium end osseous implants. Journal of Prosthetic Dentistry 84: 522–534.

Cramton, S.E., Gerke, C., Schnell, N.F., Nichols, W.W. & Gotz, F. (1999) The intercellular adhe-€ sion (ica) locus is present in Staphylococcus aureus and is required for biofilm formation. Infection and Immunity 67: 5427–5433.

De Nardo, L., Raffaini, G., Ebramzadeh, E. & Ganazzoli, F. (2012) Titanium oxide modeling and design for innovative biomedical surfaces: a concise review. The International Journal of Artificial Organs 35: 629–641.

Dhir, S. (2013) Biofilm and dental implant: the microbial link. The Journal of Indian Society of Periodontology 17: 5–11.

Dhir, S., Paquette, D.W., Brodala, N. & Williams, R.C. (2006) Risk factors for endosseous dental implant failure. Dental Clinics of North America 50: 361–374.

Di Giulio, M., Di Bartolomeo, S., Di Campli, E., Sancilio, S., Marsich, E., Travan, A., Cataldi, A. & Cellini, L. (2013a) The effect of a silver nanoparticle polysaccharide system on streptococcal and saliva-derived biofilms. International Journal of Molecular Sciences 14: 13615–13625.

Di Giulio, M., di Giacomo, V., Di Campli, E., Di Bartolomeo, S., Zara, S., Pasquantonio, G., Cataldi, A. & Cellini, L. (2013b) Saliva improves Streptococcus mitis protective effect on human gingival fibroblasts in presence of 2-hydroxyethylmethacrylate. Journal of Materials Science Materials in Medicine 24: 1977–1983.

Diaz, P.I. (2012) Microbial diversity and interactions in subgingival biofilm communities. Frontiers of Oral Biology 15: 17–40.

Elemek, E. & Almas, K. (2014) Peri-implantitis: etiology, diagnosis and treatment: an update. The New York State Dental Journal 80: 26–32.

Faeda, R.S., Tavares, H.S., Sartori, R., Guastaldi, A.C. & Marcantonio, E., Jr. (2009) Evaluation of titanium implants with surface modification by laser beam. Biomechanical study in rabbit tibias. The Brazilian Oral Research 23: 137–143.

Foster, J. & Kolenbrander, P. (2004) Development of multispecies oral bacterial community in a saliva-conditioned flow cell. Applied and Environmental Microbiology 70: 4340–4348.

Gaggl, A., Schultes, G., Muller, W.D. & K€ €archer, H. (2000) Scanning electron microscopical analysis of laser-treated titanium implant surfaces-a comparative study. Biomaterials 21: 1067–1073.

Grenier, D. (1992) Nutritional interactions between two suspected periodontopathogens, Treponema denticola and Porphyromonas gingivalis. Infection and Immunity 60: 5298–5301.

Grossner-Schreiber, B., Griepentrog, M., Haustein,€ I., Muller, W.D., Lange, K.P., Briedigkeit, H. &€ Gobel, U.B. (2001) Plaque formation on surface€ modified dental implants. An in vitro study. Clinical Oral Implants Research 12: 543–551.

Hallgren, C., Reimers, H., Chakarov, D., Gold, J. & Wennerberg, A. (2003) An in vivo study of bone response to implants topographically modified by laser micromachining. Biomaterials 24: 701–710.

Hall-Stoodley, L. & Stoodley, P. (2009) Evolving concepts in biofilm infections. Cellular Microbiology 11: 1034–1043.

Hsu, Y.T., Mason, S.A. & Wang, H.L. (2014) Biological implant complications and their management. Journal of the International Academy of Periodontology 16: 9–18.

Jefferson, K.K. (2004) What drives bacteria to produce a biofilm? FEMS Microbiology Letters 236: 163–173.

Jung, R.E., Pjetursson, B.E., Glauser, R., Zembic, A., Zwahlen, M. & Lang, N.P. (2008) A systematic review of the 5-year survival and complication rates of implant-supported single crowns. Clinical Oral Implants Research 19: 119–130.

Katsikogianni, M. & Missirlis, Y.F. (2004) Concise review of mechanisms of bacterial adhesion to biomaterials and of techniques used in estimating bacteria-material interactions. European Cells & Materials 8: 37–57.

Lang, N.P., Berglundh, T. & Working Group 4 of Seventh European Workshop on Periodontology (2011) Periimplant diseases: where are we now?Consensus of the Seventh European Workshop on periodontology. Journal of Clinical Periodontology 11: 178–181.

Li, J., Liao, H., Fartash, B., Hermansson, L. & Johnsson, T. (1997) Surface dimpled commercially pure titanium implant and bone ingrowth. Biomaterials 18: 691–696.

Liu, Y. & Zhao, Q. (2005) Influence of surface energy of modified surfaces on bacterial adhesion. Biophysical Chemistry 117: 39–45.

Lohmann, C.H., Andreacchio, D., Koster, G., Car-€ nes, D.L., Jr, Cochran, D.L., Dean, D.D., Boyan, B.D. & Schwartz, Z. (2001) Tissue response and osteo induction of human bone grafts in vivo. Archives of Orthopaedic and Trauma Surgery 121: 583–590.

Meyer, U., Buchter, A., Wiesmann, H.P., Joos, U. &€ Jones, D.B. (2005) Basic reactions of osteoblasts on structured material surfaces. European Cells & Materials 9: 39–49.

Mysak, J., Podzimek, S., Sommerova, P., Lyuya-Mi, Y., Bartova, J., Janatova, T., Prochazkova, J. & Duskova, J. (2014) Porphyromonas gingivalis: major periodontopathic pathogen overview. Journal of Immunology Research 2014: 476068.

Periasamy, S. & Kolenbrander, P.E. (2009) Mutualistic biofilm communities develop with Porphyromonas gingivalis and initial, early, and late colonizers of enamel. Journal of Bacteriology 191: 6804–6811.

Persson, G.R. & Renvert, S. (2014) Cluster of bacteria associated with peri-implantitis. Clinical Implant Dentistry and Related Research 16: 783–793.

Quirynen, M. & Bollen, C.M. (1995) The influence of surface roughness and surface-free energy on supra- and sub-gingival plaque formation in man. A review of the literature. Journal of Clinical Periodontology 22: 1–14.

Quirynen, M., De Soete, M. & van Steenberghe, D. (1999) Intra-oral plaque formation on artificial surfaces. In: Lang, N.P., Karring, T. & Lindhe, J., eds. Proceedings of the 3rd European Workshop on Periodontology, 102–129. Berlin: Quintessence Books.

Quirynen, M., De Soete, M. & van Steenberghe, D. (2002) Infectious risks for oral implants: a review of the literature. Clinical Oral Implants Research 13: 1–19.

Rupp, F., Scheideler, L., Rehbein, D., Axmann, D. & Geis-Gerstorfer, J. (2004) Roughness induced dynamic changes of wettability of acid etched titanium implant modifications. Biomaterials 25: 1429–1438.

Sammons, R.L., Lumbikanonda, N., Gross, M. & Cantzler, P. (2005) Comparison of osteoblast spreading on micro-structured dental implant surfaces and cell behavior in an explant model of osseous integration. A scanning electron microscopic study. Clinical Oral Implants Research 16: 657–666.

Shibli, J.A., Melo, L., Ferrari, D.S., Figueiredo, L.C., Faveri, M. & Feres, M. (2008) Composition of supra- and subgingival biofilm of subjects with healthy and diseased implants. Clinical Oral Implants Research 19: 975–982.

Soboyejo, W.O., Nemetski, B., Allameh, S., Marcantonio, N., Mercer, C. & Ricci, J. (2002) Interactions between MC3T3-E1 cells and textured Ti6Al4V surfaces. Journal of Biomedical Materials Research Part B: Applied Biomaterials 62: 56– 72.

Stanley, N.R. & Lazazzera, B.A. (2004) Environmental signals and regulatory pathways that influence biofilm formation. Molecular Microbiology 52:

917–924.

Subramani, K., Jung, R.E., Molenberg, A. & Hammerle, C.H. (2009) Biofilm on dental implants: a review of the literature. The International Journal of Oral & Maxillofacial Implants 24: 616–626.

Tribble, G.D., Kerr, J.E. & Wang, B.J. (2013) Genetic diversity in the oral pathogen Porphyromonas gingivalis: molecular mechanisms and biological consequences. Future Microbiology 8: 607–620.

Zhao, G., Raines, A.L., Wieland, M., Schwartz, Z. & Boyan, B.D. (2007) Requirement for both micron and submicron scale structure for synergistic responses of osteoblasts to substrate surface energy and topography. Biomaterials 28:

2821–2829.

Zhao, G., Zinger, O., Schwartz, Z., Wieland, M., Landolt, D. & Boyan, B.D. (2006) Osteoblast-like cells are sensitive to submicron-scale surface structure. Clinical Oral Implants Research 17: 258–264.

Zitzmann, N.U. & Berglundh, T. (2008) Definition and prevalence of peri-implant diseases. Journal of Clinical Periodontology 35(8 Suppl): 286–291.

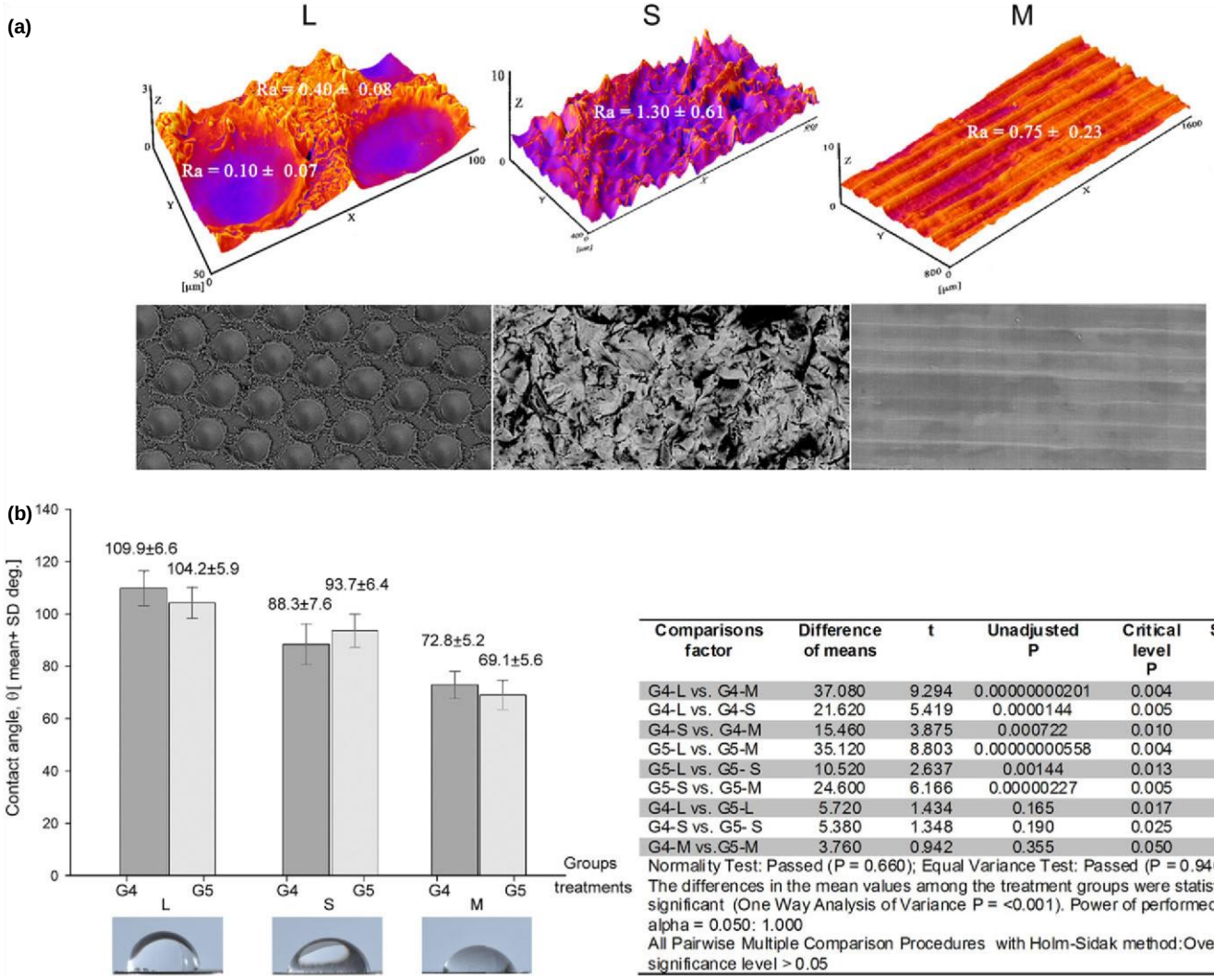

Comparisons factor	Difference of means	t	Unadjusted P	Critical level P	Significant ?
G4-L vs. G4-M	37.080	9.294	0.00000000201	0.004	Yes
G4-L vs. G4-S	21.620	5.419	0.0000144	0.005	Yes
G4-S vs. G4-M	15.460	3.875	0.000722	0.010	Yes
G5-L vs. G5-M	35.120	8.803	0.00000000558	0.004	Yes
G5-L vs. G5- S	10.520	2.637	0.00144	0.013	Yes
G5-S vs. G5-M	24.600	6.166	0.00000227	0.005	Yes
G4-L vs. G5-L	5.720	1.434	0.165	0.017	No
G4-S vs. G5- S	5.380	1.348	0.190	0.025	No
G4-M vs.G5-M	3.760	0.942	0.355	0.050	No

Normality Test: Passed (P = 0.660); Equal Variance Test: Passed (P = 0.940)
The differences in the mean values among the treatment groups were statistically significant (One Way Analysis of Variance P = <0.001). Power of performed test with alpha = 0.050: 1.000
All Pairwise Multiple Comparison Procedures with Holm-Sidak method:Overall significance level > 0.05

Fig. 1. Surface roughness (Ra) for the different surface topographies (a). (L) laser-treated; (S) sandblasted; (M) machined. SEM images at original magnification: 10009. Static contact angles with sessile drop method (b).

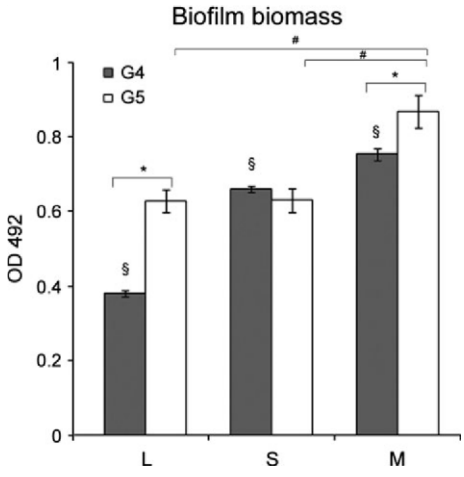

Fig. 2. Quantitative assessment of Porphyromonas gingivalis ATCC33277biofilmondifferentimplantsurfacetopographies and materials. (L) laser-treated; (S) sandblasted;

(M) machined. G4, Ti and G5, Ti-6Al-4V alloy. Significantly different ($P < 0.05$);(§)significantdifferencesamongG4-L-S-M;(*)significant differences between G4-L and G5-L, G4-M and G5-M; (#) significantdifferencesbetweenG5-LandG5-M,G5-SandG5-M.

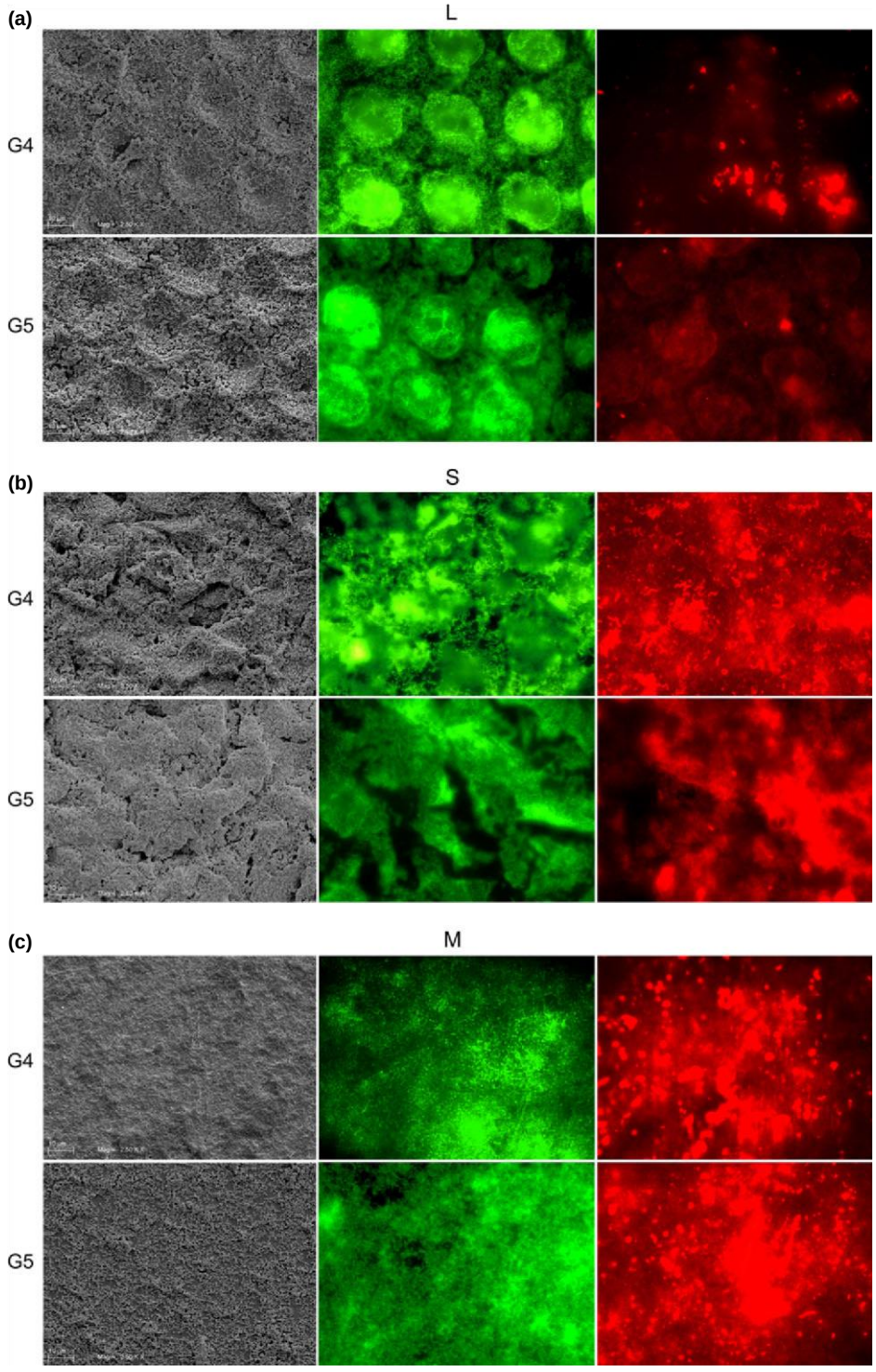

Fig. 3. Representative images of Porphyromonas gingivalis ATCC 33277 adhesion on different implant surface topographies and materials. Panel a: laser-treated surface, G4 and G5 materials; Panel b: sandblasted surface, G4 and G5 materials; Panel c: machined surface, G4 and G5 materials. The bacterial distribution was shown by SEM (left column, original magnification: 25009); the cell viability was shown by fluorescence with live/dead stain (middle column, original magnification: 10009), and the polysaccharides production was shown by fluorescence with rhodamine-conA stain (right column, original magnification: 10009). Most of the bacteria

retained on the specimen surface appeared to be alive (green intensity of middle column), while the amount of the matrix present in the biofilm was red stained (right column).

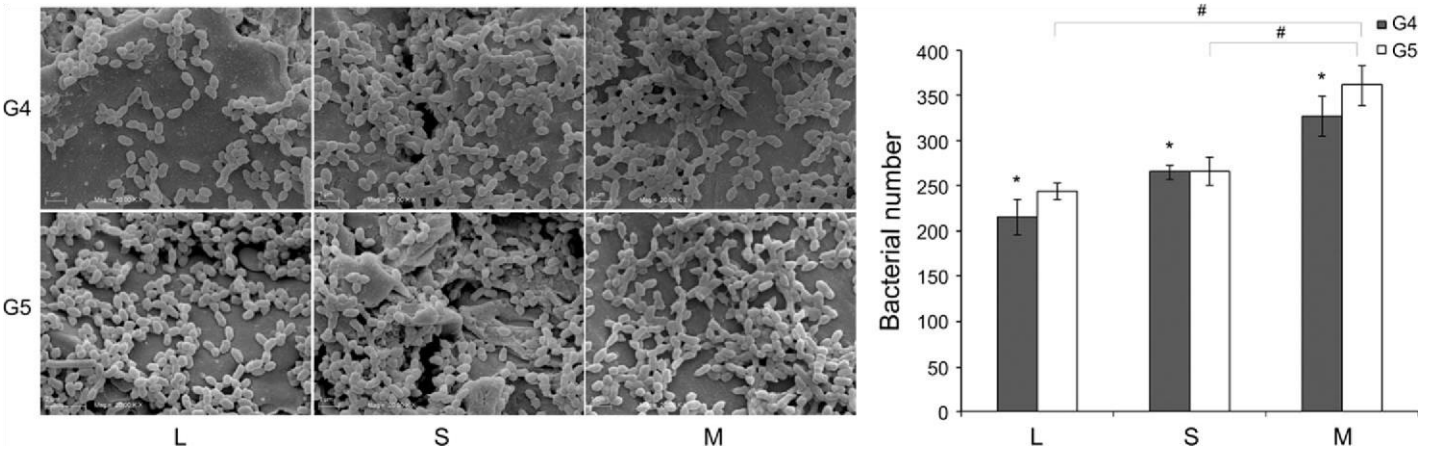

Fig. 4. Porphyromonas gingivalis ATCC 33277 cells adhered on different implant surface topographies and materials. Left: representative images by SEM (original magnification: 20,0009). Right: total cell numbers (L) laser-treated; (S) sandblasted; (M) machined. G4, Ti and G5, Ti-6Al-4V alloy. (*) Significant differences among G4-L-S-M; (#) signifi-

cant differences between G5-L and G5-M, G5-S and G5-M.